STUDIES OF GRAIN BOUNDARIES IN MELT TEXTURED $YBa_2Cu_3O_X$

B. W. Veal, H. Claus, Lihua Chen and A. P. Paulikas

Materials Science Division, Argonne National Laboratory, Argonne Illinois 60439-4830

ABSTRACT

[001] tilt grain boundaries were studied in bi-crystal samples of melt textured $YBa_2Cu_3O_x$. Grain boundary critical current densities J_{CB} were obtained from SQUID magnetization measurements on ring samples that contain the grain boundary. The dependence of J_{CB} on oxygen stoichiometry and oxygen ordering were investigated and preliminary studies of grain boundary doping with selected cations, including Ca, Sr, and Bi were undertaken.

INTRODUCTION

It is well known that grain boundaries in the high Tc superconductor $YBa_2Cu_3O_x$ (YBCO) severely inhibit supercurrent flow, with losses being most severe at high grain boundary (GB) mismatch angles [1,2]. Consequently, considerable effort is being devoted to (1) develop methods for producing YBCO materials (both bulk and film) that are relatively free of GBs, especially high angle GBs, and to (2) develop methods to minimize the effect of GBs on supercurrent transport. Associated with these efforts is the ongoing scientific challenge; to determine the local structure and to understand associated electronic behavior, including those effects which influence supercurrent flow.

One approach for minimizing deleterious transport effects is to exploit GB dopants. One obvious and important GB dopant is oxygen (or oxygen vacancies) which necessarily must be properly adjusted for optimal transport performance. Another possibility is to decorate the GBs with suitable impurity atoms which might favorable affect electronic transport. Success with this approach has been reported with Ca doping of GBs [3,4].

In this study, we extensively exploit SQUID measurements on ring samples to measure the grain boundary J_C. Effects of oxygen stoichiometry are examined, as well as the role of selected cation dopants that are diffused into GBs. GBs are investigated in bulk YBCO.

It is expected that a large variety of dopant atoms might diffuse into YBCO GBs under suitable processing conditions. Further, it seems likely that these impurity atoms will generally affect supercurrent transport across the GB. The demonstration of (beneficial) GB doping with Ca has generated an interest in understanding the mechanisms which influence supercurrent transport. Hole doping [3] and strain effects in dislocation cores [5] have been proposed as controlling mechanisms. Systematic studies of dopants in YBCO GBs might provide new insights into GB doping mechanisms and could lead to new methods for minimizing the deleterious effect of GBs on supercurrent transport.

In addition to electronic effects (hole doping) and strain effects in dislocation cores, it may be that effects of vortex pinning will be important [2]. Such effects are likely to depend strongly on GB misorientation since the nature of GB vortices changes dramatically as misorientation increases. GB vortices at small angles approximate Abrikosov vortices, with relatively localized vortex cores, but convert to Josephson vortices, with ill-defined cores, at large misorientation. Thus, the effectiveness of particular defects as pinning centers is likely to vary dramatically with GB misorientation.

Some dopants might exert significant bonding effects, perhaps establishing a local oxygen coordination shell about the dopant atom. However, in order to controllably dope GBs using diffusion, it will be necessary that GB diffusion dominates over bulk diffusion or chemical attack, with attendant destruction of the YBCO structure. Presumably, strong bonding behavior will affect supercurrent transport, perhaps varying with bond strength and coordination shell.

EXPERIMENTAL

Sample Preparation

Melt-textured cylindrical YBCO monoliths were produced using a top-seeding method as described in ref 6. To obtain [001] tilt GBs, pressed powder cylindrical samples were melt-textured using two Sm123 seeds, with their c-axes aligned parallel to the axis of the cylinder. The crystals were rotated about their c-axes so that a-b planes had the desired misorientation. Simultaneous seeding, initiated at the two crystals, leads to a melt textured "bi-crystal" with the desired [001] tilt misorientation. Some of the textured samples were densified using a processing step in O_2 [6], while some were textured, in air, without the densification step.

J_{CB} Measurements on Ring Samples

Grain boundary critical current densities J_{CB} were obtained from SQUID magnetization measurements on ring samples that were core-drilled from the bi-crystal samples. Rings, with ~ 1x1 mm^2 cross section and 5 mm outer diameter, were cut so that the grain boundary plane cuts across the ring parallel to the ring axis. To acquire the SQUID measurements, a sample was cooled, in zero field, to

a temperature well below T_C, then a magnetic field was applied parallel to the ring axis and the sample was warmed at constant field. Fig. 1 displays SQUID **dc**

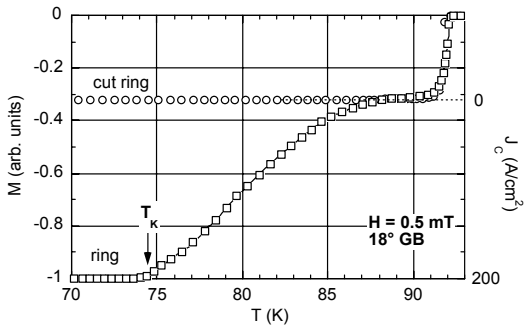

Fig. 1 Magnetic moment of a ring, containing an 18° grain boundary (see text). The data were taken on warming in a magnetic field of 0.5 mT after initially cooling in zero field to below 70 K. The right scale indicates the critical current density of the grain boundary. Also shown is the magnetic signal of the ring after it had been cut, preventing any circulating currents.

magnetization measurements taken from a ring sample that contains an 18° [001] tilt boundary.

At the lowest temperatures, where M is independent of temperature, flux is completely excluded from the ring bore. As the temperature is increased (Fig. 1), the critical current across the GB will fall, and the current that has been induced in the ring will eventually exceed the critical current across the boundary. At this point flux will begin to leak into the ring, decreasing the observed magnetization. This onset of flux penetration into the ring produces the abrupt decrease in M (T) that is clearly observed in Fig. 1 at the temperature labeled T_K (kink temperature). Considering the ring to be a single-turn solenoid, the induced current providing shielding of the ring bore can be estimated, to good approximation, from the simple expression I=D*H, where D is the outer diameter of the ring and H is the applied magnetic field [6,7]. Thus, I(A)=4*H (mT) for our ring geometry.

As the temperature is further increased above the kink temperature T_K, the shielding current flowing around the ring becomes limited by the declining critical current across the boundary and flux increasingly leaks through the GB into the bore of the ring. The nearly linear decrease in M vs. T above T_K reflects a nearly linear decrease of J_{CB} with temperature.

The plateau in M vs. T reached at about 30% of the full shielding signal indicates that the critical current in the junction has dropped to zero and the field inside the bore now almost equals the field outside. The remaining signal (i.e., at 90 K) is due to flux expulsion from the annulus, which has a transition temperature of about 92 K. The plateau in M(T) coincides with the diamagnetic

signal from the ring after a slit has been cut into the ring to prevent any circulating shielding currents [6].

RESULTS AND DISCUSSION

J_{CB} Versus Misorientation Angle

Fig. 2 shows measurements of J_{CB} vs misorientation angle for [001] tilt grain

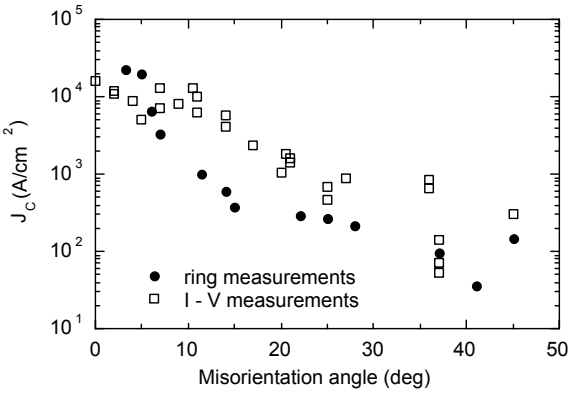

Fig. 2 Critical current at 77 K of grain boundaries versus misorientation angles (see text). Open squares are from resistivity measurements (see ref **2**). The closed circles are from ring measurements like that in Fig. 1.

boundaries with misorientations spanning the range from 0 to 45°. Open symbols, taken from the literature, are J_{CB} obtained from conventional I-V measurements [2]. Solid symbols identify data acquired using the SQUID technique. The SQUID results are generally lower. This results, in part, from a much smaller voltage criterion for the SQUID measurements [6]. Also, some of the shift might result from a depression of J_{CB} by the applied measurement field; this appears to be most important at high misorientations [8].

Dependence of GB Transport on Magnetic Field

Numerous measurements have been reported for the zero field dependence of GB J_C on misorientation angle, especially for [001] tilt GBs [2]. However, it is also the case that J_{CB} is a very strong function of magnetic field, especially for large mismatch angles and temperatures relatively close to T_C; e.g., at 77 K [8]. We note that SQUID measurements on ring samples that contain a GB are particularly convenient for field dependent studies of grain boundary J_C. For these experiments, we cool the sample in an applied field of H-δ. Then, with the sample cooled to a temperature below Tc, the field is increased to H+δ. A

shielding current will be induced to screen the 2δ incremental field. At the kink temperature, $J_C = 400*(2\delta)$ for a ring sample with a 1 mm cross section, where J_C is expressed in A/cm^2 and δ is in mT.

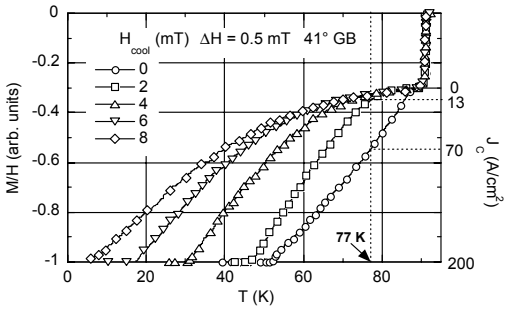

Fig. 3 Magnetic moment of a 41° grain boundary versus temperature in magnetic fields between zero and 8 mT. The data were taken on warming after initially cooling the ring in a field of H-δ to low temperature and then increasing the field to H+δ before warming, where 2δ = 0.5 mT. The right scale indicates the critical current density of the grain boundary.

Fig 3 shows M(T) for a GB with 41 degrees of misorientation when H+δ is varied from zero to 8 mT. The incremental field δ is 0.25 mT. The grain boundary J_C is shown on the right hand scale of Fig 3. Note that, at 77 K, the value of J_C falls by more than a factor of 5 as the applied field is increased from zero to 2 mT. Miller, et al. [8] observed comparably large field dependent changes in 77K measurements of transport J_C for misorientations up to 25°.

Dependence of GB Transport on Oxygen Stoichiometry

The level of oxygenation profoundly affects the superconducting and normal state properties of YBCO. However, the role of (excess or deficient) oxygen in the GBs has not been clearly established. In this study, we repeatedly process ring samples cut across [001] tilt GBs at appropriate temperatures and oxygen pressures so that the bulk oxygen stoichiometry is changed in a controlled fashion.

Fig. 4 shows T_K as a function of annealing time at 450°C, in O_2, for a 27 ° grain boundary. Measurements were made in a field of 0.5 mT. The sample was given repeated oxygenation exposures until T_K saturated at about 76 K. A treatment of 10 to 20 hrs appears to be adequate for essentially full oxygenation of the 1 mm^2 grain boundary. As Fig 4 attests, the oxygenation behavior is remarkably well behaved. No apparent damage to the GB is introduced by the repeated thermal cycling. The solid line in Fig 4 is a fit of the data to the exponential expression shown in Fig. 4 with $T_{K0} = 53$ K, $\Delta T = 23$ K and $\tau = 3.4$ h.

As expected, the oxygenation rate is strongly temperature dependent. Preliminary studies indicate that about 300 hrs are needed to fully oxygenate the

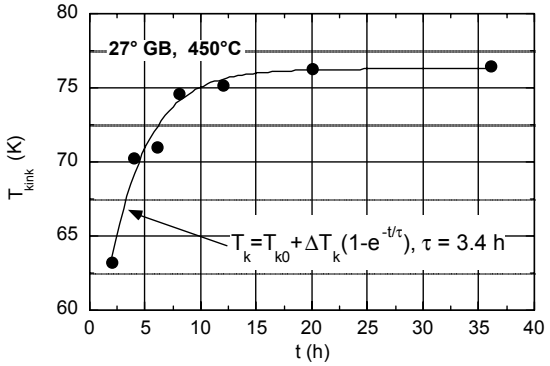

Fig. 4 Variation of the kink temperature (see Fig. 1) with oxygenation time at 450°C. The data are for a 27° grain boundary. The solid line is an exponential fit to the data.

GB at 350°C. It appears, furthermore, that J_{CB} continues to rise as the oxygenation level is increased, even as the bulk material becomes "overdoped" and T_C shows a small decline. This behavior is illustrated in Fig. 5 where measurements were taken after extended treatments at 450°C and at 350°C in O_2. J_{CB} increases as the oxygenation temperature is reduced, increasing the oxygen

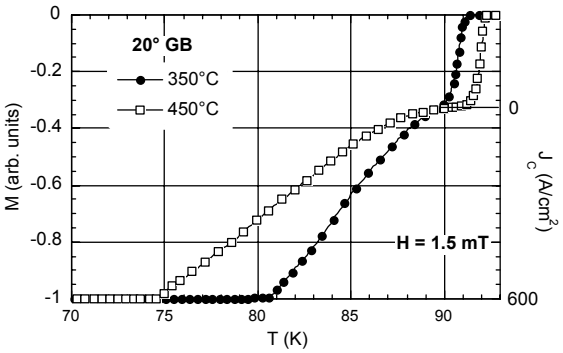

Fig. 5 Magnetic moment in 1.5 mT of a ring containing a 20° grain boundary versus temperature, after the ring was oxygenated first at 350°C then at 450°C. The right scale indicates the critical current density of the grain boundary.

stoichiometry, while the bulk T_C declines.

It is usually the case, at temperatures well below the melting temperature, that GB diffusion is significantly faster than bulk diffusion. Thus we expect the GB to become oxygenated more rapidly than the surrounding bulk. However, in order to

make measurements such as those in Fig 4, it must be that oxygenation into the bulk is sufficiently fast so that an oxygenated shell of thickness exceeding the superconducting penetration depth is achieved. If bulk pinning is strong, the SQUID shielding measurement will show complete flux exclusion giving a full diamagnetic signal even though the central region of the ring might remain nonsuperconducting. In order to detect the full value of I_C across the GB, it must also be that the bulk material, in proximity to the GB, is also sufficiently oxygenated to carry the transmitted I_C to the ring surface. This internal bulk oxygenation that occurs in close proximity to the GB is supplied through the fast

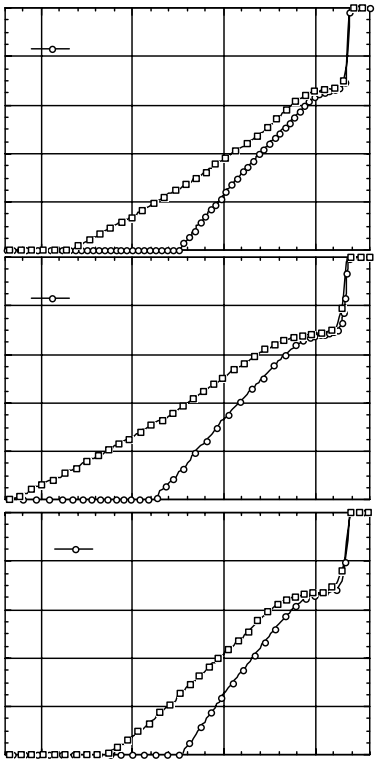

Fig. 6 Magnetic moment in 0.5 mT of three rings all containing a 21° grain boundary. Each panel shows one ring in the as made state (oxygenated at 450°C) and after heat treatment at 800°C for 4 hours followed by a 450°C oxygenation. The rings in panel **A** and **B** were immersed in $CaCO_3$ and Sm_2O_3 powders respectively during the 800°C treatment. The ring in panel **C** was given the same 800°C treatment in air.

diffusion GB path. The ring surface must also be sufficiently oxygenated to carry the full I_C. For the data of Fig 4, the bulk was sufficiently oxygenated to carry the

full I_C transmitted across the GB; i.e., the full diamagnetic signal from the bulk was observed after each stage of oxygenation.

The data in Fig. 4 indicate that the bi-crystal samples can be repeatedly processed with thermal treatments up to about 500°C, apparently without damage or significant change to the GB. Thermal excursions between the process temperature and cryogenic temperatures, where measurements are taken, apparently do not damage the GBs. The GB structure (aside from effects of oxygenation) apparently remains remarkably stable. However, nonreversible behavior is often observed when process temperatures exceed 500-600°C.

Nonreversible Behavior

GB transport is apparently affected by the thermal history of the sample, especially if it has experienced extended time treatments in the temperature range of 600-900°C. Consequently, if a diffusion experiment is conducted in this temperature range, it is mandatory that reference samples be given identical heat treatments, but without exposure to the GB diffusant.

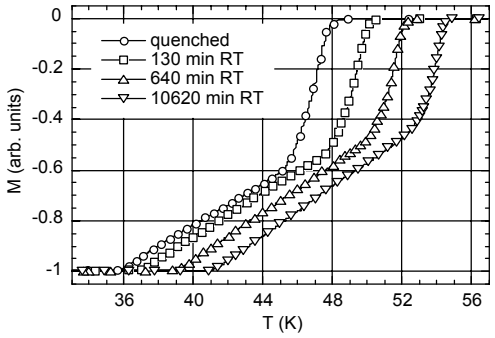

Fig. 7 Magnetic moment in 0.5 mT of a ring, containing an 11° grain boundary. The oxygen concentration was adjusted to 6.44 (see text). The ring was then equilibrated at 120°C and quenched into chilled ethanol followed by room temperature anneals for the time intervals as indicated.

A simple illustration is shown in Fig 6, where M(T) data are presented for three -crystal samples cut from the same dual seeded 21° GB. The samples were treated for 116 hrs at 450°C in flowing O_2 and M(T) data were recorded [open circles]. The samples were subsequently treated [open squares] for 4 hrs at 800°C in air while immersed (A) in a powder of $CaCO_3$, and (B) in a powder of Sm_2O_3. Sample (C) was simply reprocessed, as a 'placebo' standard for the same 4 hr air exposure at 800°C. All samples were given a final oxygenation treatment at 450°C for 95 hrs to return the bulk T_C to its optimal value.

Note that all three rings have quite similar GB J_C's at 77 K, both before and after the thermal processing. The behavior of the reference sample is nearly equivalent to the cation-treated samples, strongly suggesting that no significant concentration of impurity cations has diffused into the GBs under these processing conditions, even though J_C values across the GBs have changed quite dramatically.

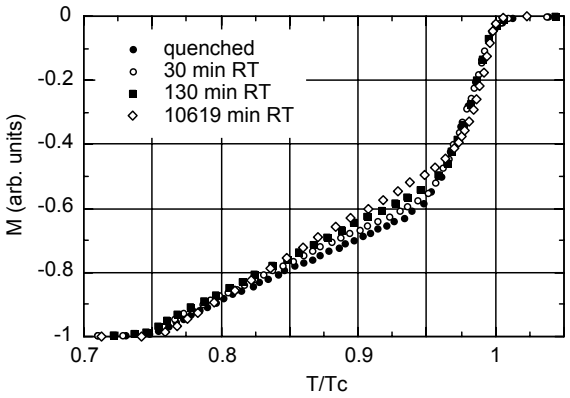

Fig. 8 Same measurements as in Fig. 7 but with the temperature scale normalized to T_C.

This behavior might result from altered GB pinning caused by the 800°C heat treatment. The reduced values of J_{CB} suggest that some pinning defects have been annealed out. Notably, a very similar alteration of the pinning behavior was encountered for each of the three samples. In any case, the thermally induced change does not require the presence of a GB diffused cation impurity. This illustrates the need to apply extreme care in interpreting the results of GB diffusion experiments. Also, it emphasizes that thermal history is likely to play a significant role in the GB transport.

Oxygen Ordering

The state of order of oxygen atoms in the chain layer of oxygen deficient YBCO can have a profound influence on the superconducting and normal state properties of the bulk material [9]. Further, the state of order is strongly dependent on temperature. A disordered state will rapidly anneal, even at room temperature, with an associated rise in the superconducting T_C. The properties changes are consistent with, and have been attributed to, a change in the level of hole doping resulting from an increase in the concentration of 2-coordinated (monovalent) Cu atoms located in the chains [10].

We have investigated the effect, on the grain boundary J_C, resulting from changing the state of order of oxygen vacancies residing in the chain layer of

YBCO. This experiment has an apparent analog in the study of GB doping with Ca. It is argued that Ca^{2+} doping increases the J_C as a consequence of substituting on Y^{3+} sites thereby increasing the hole doping at GBs [3]. Of course, doping associated with ordering occurs throughout the material, but may also affect GB properties [11].

M(T) measurements were made on a sample with stoichiometry x = 6.44, obtained by annealing for 190 hrs at 500°C in a flowing gas stream consisting of 0.17 % O_2 in N_2, followed by a quench to liquid nitrogen. To disorder the chain oxygens, the sample was then heated to 120°C and, after 10 min, was quenched into chilled ethanol. Then a series of M(T) measurements were recorded as the sample annealed at room temperature.

Fig 7 shows the M(T) data recorded after specified time intervals as room temperature annealing proceeded. The kink temperature, identifying a fixed value of J_C, increases with the rising T_C. Fig 8 shows the M(T) plotted vs the reduced temperature T/T_C. The fixed value of the kink temperature in the reduced temperature plot suggests that the GB J_C is primarily controlled by the value of T_C without significant effects that could be attributed to changes within the grain boundary. Thus, to first order, this doping mechanism does not appear to play an important role in influencing GB transport.

Cation Doping

Recent studies on thin film samples have demonstrated that Ca is an effective GB dopant to increase the supercurrent density across GBs in YBCO [3,4]. It is argued that Ca^{2+} ions substitute on Y^{2+} sites thereby increasing the hole concentration which serves to improve GB coupling increasing the GB J_C. Strain effects resulting from dopant ions in GB cores may also play an important role in influencing J_C [4,5].

The mechanisms responsible for improvement of GB transport resulting from Ca doping are not known. Consequently, it would appear to be worthwhile to investigate the effects caused by GB doping, for a variety of dopant ions, with variations in ion size, valence state and electro-negativity.

Using bi-crystal GBs produced with dual seeding techniques in melt textured bulk samples, we are searching for thermal treatment conditions that will permit controlled doping of the artificial GBs with selected cation dopants. If dopants can be placed within GB cores without reacting with the YBCO to form separate phases, the possibility exists that GB coupling can be improved so that supercurrent losses across GBs can be substantially reduced. Successful GB doping strategies could then be used for improving J_C in melt textured bulks and in coated conductors, both of which contain small angle GBs. Alternatively, with

successful GB doping, it might be possible to utilize materials which contain larger mismatch angles than can presently be tolerated.

Ca doping: Since GB doping with Ca has been successfully demonstrated in film samples, we have attempted to achieve doping, and to demonstrate J_C enhancement, by diffusing Ca atoms into GBs prepared in MTG material. Results

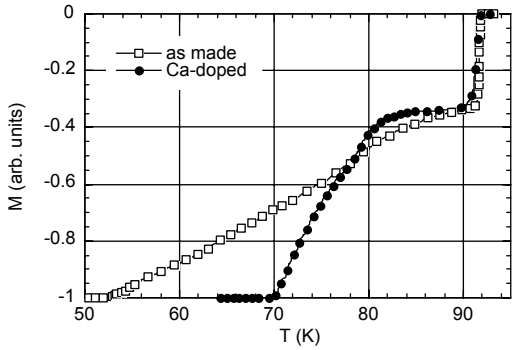

Fig. 9 Magnetic moment in 0.15 mT of a ring, containing a 38° grain boundary before and after Ca – doping at 970°C (see text). In both states the ring was fully oxygenated at 450°C.

of an apparently successful doping strategy are shown in Fig 9 for a 38° [001] tilt bi-crystal. The curve marked 'as-made' was measured before the ring sample was exposed to a Ca source. It was simply given an oxygenation treatment for 9 days at 450°C in flowing O_2. Following this measurement, the sample was immersed in $CaCO_3$ powder and was treated for 60 hrs at 970°C, followed by a 30 hr homogenization anneal in air, again at 970°C. The sample was then oxygenated for 9 days at 450°C in flowing O_2.

Fig 9 shows that, at temperatures below ~ 77 K, J_C is appreciably enhanced

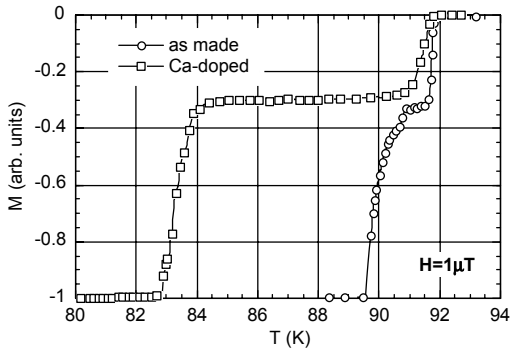

Fig. 10 Same as in Fig. 9 but in a field of 1 μT.

after the Ca treatment; at 70 K, J_C has approximately doubled. Fig. 10 shows M(T) measurements, taken at 1 μT, for both the original and Ca doped samples. At the kink temperature (both curves), the current density is about 0.4 A/cm^2. For the original sample, T_K appears at ~ 89.5 K and J_C falls to zero at the T_C of the bulk, near 91.5 K. For the doped sample, T_K has fallen to about 83 K. By ~ 84 K, the ring carries essentially no circulating shielding supercurrent. This suggests that the GB is somewhat excessively doped with Ca. Probably the bulk material in close proximity to the GB has become doped with Ca reducing its T_C to ~ 85 K. A slight broadening of the bulk transition is also apparent, possibly resulting from Ca doping, with some T_C depression, in the outer surface of the ring. A more carefully optimized heat treatment, utilizing Ca doping, would probably yield further improvement in the GB J_C, especially for operation at 77 K. It might also be, of course, that such beneficial effects will vary with misorientation angle.

Sr doping: Sr is of interest as a GB dopant because, like Ca, it is divalent, but it has a larger ionic radius which prevents substitution on the Y site. Sr can substitute on the Ba site, but since both Sr and Ba are divalent, no significant change in hole doping is expected. If GB decoration with Sr can be accomplished, and if there is a discernable effect on J_C, this might be taken as evidence that strain effects in GB cores provide a mechanism for controlling GB supercurrent transport.

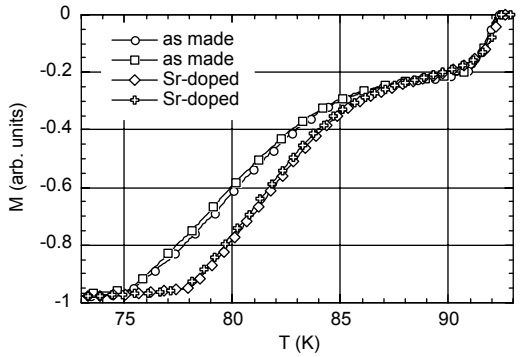

Fig. 11 Magnetic moment in 0.4 mT of four ceramic YBCO rings, two as made and two after Sr-doping (see text). All rings were fully oxygenated at 450°C before the measurement.

Our studies showed that the doping behavior was complex, generally showing minimal improvement in GB J_C. However, there did appear to be circumstances in which significant improvement could be realized. Low quality GBs; e.g., GBs

with unusually low values of J_C, were typically improved, sometimes dramatically, with Sr treatment. Even open circuit rings could generally be restored to typical $J_C(\theta)$ values after Sr treatment. Occasionally, however, improvements were observed in these low quality GBs, even after a heat treatment with no Sr source available.

Dense polycrystalline ceramic ring samples [6] showed a small but apparently

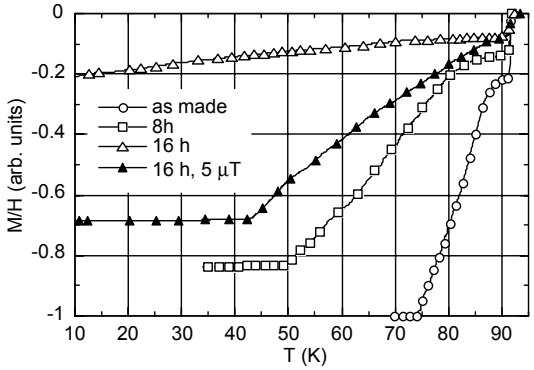

Fig. 12 Magnetic moment in 0.5 mT of a ring containing a 26° grain boundary, befor and after Bi – doping at 800°C (see text). Before each measurement the ring was fully oxygenated at 450°C. For the 16 h treatment the critical current of the boundary is too small to show a kink. For this state, data were taken also at 5μT.

robust improvement after Sr treatment. Fig 11 shows measurements on four ring samples, two of which received Sr treatment (60 hrs at 970°C while immersed in $SrCO_3$ powder) two did not (all oxygenations at 450°C). At 77 K, an improvement of ~ 30% in J_C is observed. Note that, for the ceramic ring samples, a well defined and highly reproducible kink temperature is observed. This defines the weakest link for flux entry into the ring core. The J_C for transport across this complex path of linked GBs traversing the sample is remarkably similar for the different rings.

Bi doping: Fig. 12 shows M(T) for a ring containing a 26° GB before (open circles) and after treatments at 800 C in Bi_2O_3 powder. The ring was given two successive 8 hr treatments, with magnetization measurements acquired after each treatment. At 800°C, Bi_2O_3 slowly attacks the YBCO, generating an abrupt decomposition front as attack proceeds. The decomposed material is nonsuperconducting. After the first treatment (open squares), the diamagnetic signal from the bulk of the ring (i.e., the signal at 90 K), is about 60% of the original signal. This signal is approximately proportional to the undecomposed volume.

Below the kink temperatures, the circulating currents are nominally the same for the treated and untreated rings (the currents are induced by the 0.5 mT applied field). However, the grain boundary J_C is dramatically smaller after the Bi treatments. We see that, at 75 K, the grain boundary J_C has fallen, after the first Bi treatment, to about 25 % of the pretreatment value (compared to the 60% bulk diamagnetic signal). After the second (16 hr) Bi treatment, the bulk signal (at 90 K) has fallen to about 25 % of the original signal, while the grain boundary J_C (e.g., at 75 K) has fallen to about 2.5 % of its original value. The solid triangles show M measured at 5μT.

Thus, the current circulating around the ring falls much more rapidly than the bulk signal, indicating that the rate of Bi diffusion into the GB exceeds the progression rate of the attack front at the bulk. Clearly, Bi doping of the GB severely depresses supercurrent transport. Because of the strong tendency for chemical attack, it seems plausible that an isolated Bi ion residing in the GB might cause severe distortions of the local atomic structure and the electronic charge distribution. The net result is reduced GB coupling.

SUMMARY

Grain boundary supercurrent transport was studied in melt textured bi-crystal samples containing [001] tilt grain boundaries. J_{CB} data were obtained from SQUID magnetization measurements on ring samples containing a GB. The study included investigation of J_{CB} vs misorientation angle, the field dependence of J_{CB} in small externally applied fields, dependence of J_{CB} on oxygen stoichiometry and oxygen ordering. Preliminary studies of grain boundary doping with selected cations, including Ca, Sr, and Bi were undertaken. Additional systematic studies with related dopants, coupled with atomistic calculations, might provide a clearer picture of the role of dopant cations in grain boundaries and their influence on superconducting coupling.

ACKNOWLEDGEMENTS

This work is partially supported by the U.S. Department of Energy, Basic Energy Sciences-Materials Sciences-Metals, Ceramic and Engineering Sciences and Energy Efficiency and Renewable Energy, Superconductivity Program for Electric Systems, under contract W-31-109-ENG-38.

REFERENCES

[1]D. Dimos, P. Chaudhari and J. Mannhart, "Orientational Dependence of Grain-Boundary Critical Currents in $YBa_2Cu_3O_{7-x}$ bi-Crystals," *Phys. Rev. B* **41**, 4038-4041 (1990).

[2]K. E. Gray, M. B. Field and D. J. Miller, "Explanation of low critical currents in flat, bulk versus meandering, thin-film [001] tilt bi-crystal grain boundaries in $YBa_2Cu_3O_7$", Phys. Rev. B**58**, 9543 (1998), and refs. therein.
[3]G. Hammerl, A. Schmehl, R.R. Schulz, B. Goetz, H. Bielefeldt, C.W.Schneider, H. Hilgenkamp and J. Mannhart, "Enhanced Supercurrent Density in Polycrystalline $YBa_2Cu_3O_{7-x}$ at 77 K from Calcium Doping of Grain Boundaries," *Nature* **407**, 162-164 (2000).
[4]K. Guth, H. U. Krebs, H. C. Freyhardt and Ch. Jooss, "Modification of transport properties in low-angle grain boundaries via calcium doping of thin films", Phys. Rev. B**64**, 140508 (2001), and refs. therein.
[5]A. Gurevich and E. A. Pashitskii, "Current transport through low-angle grain boundaries in high-temperature superconductors", *Phys. Rev.* **B57**, 13878-13893 (1998).
[6]H. Claus, U. Welp, H. Zheng, L. Chen, A. P. Paulikas, B. W. Veal, K. E. Gray, G. W. Crabtree, "Critical Current across Grain Boundaries in Melt-Textured YBCO Rings," *Phys. Rev. B* **64**, 144507-1-9 (2001).
[7]H. Zheng, H. Claus, L. Chen, A.P. Paulikas, B.W. Veal, B. Olsson, A. Koshelev, J. Hull, and G.W. Crabtree, "Transport currents measured in ring samples: a test of superconducting weld," *Physica* C **350**, 17-23 (2001).
[8]D. J. Miller, V. R. Todt, M. St. Louis-Weber, X. F. Zhang, D. G. Steel, M. B. Field and K. E. Gray, "Microstructure and transport behavior of grain boundaries in $YBa_2Cu_3O_y$: a comparison between thin films and bulk bi-crystals", Mat. Sci. and Eng. B**53**, 125 (1998).
[9]B. W. Veal, A. P. Paulikas, H. You, H. Shi, Y. Fang, and J. W. Downey, "Observation of Temperature-Dependent Site Disorder in $YBa_2Cu_3O_{7-\delta}$ Below 150°C", Phys. Rev. B **42**, 6305 (1990).
[10]B. W. Veal and A. P. Paulikas, "Dependence of Hole Concentration on Oxygen Vacancy Order in $YBa_2Cu_3O_{7-\delta}$: A Chemical Valence Model", Physica C **184**, 321 (1991).
[11]B. H. Moeckly, D. K. Lathrop, and R. A. Buhrman, "Electromigration study of oxygen disorder and grain-boundary effects in $YBa_2Cu_3O_{7-\delta}$ thin films", Phys. Rev. B **47**, 400 (1993).